The study of the influence of morphology anisotropy of clusters of superparamagnetic nanoparticle on magnetic hysteresis by Monte Carlo simulations

Rong Fu, Clive Roberts, Yuying YAN*

*Corresponding author: Tel.: +44 (0) 115 951 3168; Fax: +44 (0) 115 95 13159;
Email: yuying.yan@nottingham.ac.uk
Energy & Sustainability Research Division, Faculty of Engineering, University of Nottingham, University Park, Nottingham NG7 2RD, UK

ABSTRACT Nowadays, extensive attentions have been focussed on the study of induction heating implanted magnetic nanoparticle under AC magnetic field for cancer hyperthermia treatment. Colloidal cluster composed of superparamagnetic nanoparticle has shown great potential for efficient hyperthermia heating. However, the relationship between cluster properties and heating efficiency is not clear. In this work, we investigate the influence of morphology anisotropy of cluster of superparamagnetic nanoparticle on magnetic hysteresis by Monte Carlo simulation. Five kinds of clusters with different shapes and structure are studied. We find that the morphology anisotropy of cluster changes the magnetic loss by affecting the tendency of cluster to remain magnetically aligned with the field orientation. A large aspect ratio of the length of cluster along the field orientation to the width perpendicular to the orientation can increase the amount of energy converted per cycle significantly. Lacking morphology anisotropy will make the magnetic hysteresis of cluster numb to the manipulation of cluster properties.

Keywords: hyperthermia; Superparamagnetic; dipole interaction; Monte Carlo; Cluster.

1. Introduction

Magnetic hyperthermia based on induction heating of magnetic nanoparticle (MNP) under AC magnetic field is emerging as a new frontier in the field of cancer therapy. Recently, the studies of this field calls on reducing the field frequency f and amplitude H_0 during the treatment.[1, 2] It is because that in addition to the expected heating generated by MNPs, alternating magnetic field also causes non-selective heating of both cancerous as well as healthy tissue by eddy currents.[3] However, any reduction in either f or H_0 leads to a sharp decrease in heating efficiency[1,4-7]. To reinforce the heating ability of MNP, numerous efforts have been made to investigate the effects of particle's properties on heating efficiency, including the particle size[4,5,8-10], size distribution[4, 5], composition[10-12], and shape[13-15]. Lots of works chose ferromagnetic MNPs for hyperthermia heating, because the difficulty to turn over the coercivity of particle will trigger the production of heat through hysteresis losses, significantly enlarging the amount of energy converted per field cycle (also-called loss per cycle).[14, 16-18] However, the onset of hysteresis loss of large particles demands a threshold field amplitude which must be stronger than the coercivity of particle.[19, 20] Although it doesn't requires high field intensity for the heat generation of superparamagnetic nanoparticles (SMNP) through delay in relaxations, the limited loss per cycle lows down their heat efficiency. [19, 20]

Now, people start to use colloidal clusters composed of MNP for magnetic hyperthermia. Hayashi *et al.*[21] reported that the heating efficiency increased by 50% after controllably assembling magnetite nanoparticle into

colloidal clusters. Nonetheless, several evidences show that the heating efficiency does not always increase after assembling the particles or raising the scale of clustering.[22, 23] The alteration of heating efficiency after dense packing of MNPs is generally attributed to the influence of inter-particle dipole interactions among the particles on the magnetic hysteresis of particle ensemble. [24-26] It is well known that the potential energy of dipole–dipole interaction heavily depends on the relative position of two MNPs and the distance between them.[27] So, it is natural to infer that the change in the structure or shape of MNP assembly may affect the magnetic hysteresis. Mehdaouithe *et al.*[28] found that inter-particle dipole interactions could generate an uniaxial magnetic anisotropy throughout the whole MNP assembly, increasing the loss per cycle, when the assembly possessed high morphology anisotropy, *i.e.* chain or cylinder.

At present, it is available to obtain a variety of MNP clusters with different shapes in experiment.[29, 30] However, it is still too early to control the heating efficiency of MNP cluster by adjusting the properties of cluster, because the relationship between them is not clear. In this work, we investigate, by Monte Carlo simulations, the effect of morphology anisotropy of SMNP clusters on the magnetic hysteresis. The clusters with three kinds of regular shapes are investigated, including chain cluster, cylinder cluster, and cube clusters possessing simple cubic, FCC and defected lattice. We find that the morphology anisotropy controls the magnetic hysteresis of cluster via changing the tendency of cluster to remain magnetically aligned with the field orientation. As the aspect ratio of length of cluster in the field orientation to the width perpendicular to the field orientation, the particles are more inclined to remain aligned with field via dipole couplings, intensifying the magnetic hysteresis of cluster. Lacking the morphology anisotropy, the heating abilities of cube clusters maintain the same regardless of the type of lattice. The introduction of defect to the lattice of cube cluster can alter the heating efficiency within a range, but the probability of increasing the efficiency is nearly equal to that of damaging the efficiency.

2. Modelling and simulation

In the physical model applied in our numerical simulation, the clusters are built upon single-domain magnetic nanoparticles with an effective uniaxial magnetic anisotropy, which is assumed to originate exclusively from the magnetocrystalline. All particles are ideal sphere in shape and covered by a stabilizer layer with thickness of 1 nm. The radius of magnetic fraction is kept as constant at 5 nm. The magnetic properties of particle referenced published data of magnetite nanoparticle: is 9000 J/m^3 and is 446 kA/m[10]. The easy axis and magnetic moments of particles are oriented randomly in the three-dimensional space. We also assumed that every particle has uniform magnetization and composition, and all its atomic moments rotating coherently. So, the magnetic moment $\vec{\mu}_i$ of particle i can be defined as $\vec{\mu}_i = M_d V_i \vec{s}_i$, where M_d is domain magnetization of magnetic material and supposed to be temperature-independent, V_i is the magnetic volume of particle i and kept as constant, and $\vec{s}_i$ is the unit vector of $\vec{\mu}_i$. The energy model of cluster system is the same as reported work[31], including three major sources: anisotropy E_A caused by magnetic crystalline anisotropy of particle, Zeeman E_H resulting from the interaction with magnetic field and dipolar interaction E_D . The uniaxial anisotropy $E_A^{(i)}$ of each particle i is given by,

$$E_A^{(i)} = -K_{eff} M_d V_i (\vec{s}_i \cdot \vec{n}_i)^2 \qquad (1)$$

where K_{eff} is the magnetic anisotropy constant of particle, and $\vec{n}_i$ the unit vector along the easy axis direction. The interaction of each particle i with the applied field $\vec{H}$ is described by,

$$E_H^{(i)} = -\mu_0 M_d V_i (\vec{H} \cdot \vec{s}_i) \qquad (2)$$

where μ_0 is the vacuum permeability. The energy of dipole couplings between two particle i and j separated by $\vec{r}_{ij}$ (the distance

between the centres of particle i and j) is given as,

$$E_D^{(i,j)} = \frac{\mu_0 M_d^2 V_i V_j}{4\pi}\left[\frac{\vec{s}_i \cdot \vec{s}_j}{r_{ij}^3} - \frac{3(\vec{s}_i \cdot \vec{r}_{ij})(\vec{s}_j \cdot \vec{r}_{ij})}{r_{ij}^5}\right] \quad (3)$$

Adding up equation (1) to (3) and summing over all particles, the total energy of the cluster system is expressed as,

$$E = \sum_i E_A^{(i)} + \sum_i E_H^{(i)} + \sum_{i<j} E_D^{(i,j)} \quad (4)$$

Five kinds of SMNP clusters are studied in this work. Figure 1 shows the sample stereographic views of these five kinds of clusters. Chain, cylinder and cube cluster with simple cubic lattice are built upon 64 particles. In chain cluster, particles are arranged head to tail straight along the [001] direction. In cylinder cluster, the unit cell of simple cubic is repeated along the [001] direction. The cube cluster with simple cubic lattice contains 4 layers, each of which consists of 16 particles. The cube cluster with FCC lattice consists of 63 particles and contains 5 layers. The cube cluster with defected lattice is fabricated by omitting 16 randomly-picked particles from the structure of cube cluster with simple cubic lattice. In this way, 50000 cube clusters with defected lattice are made.

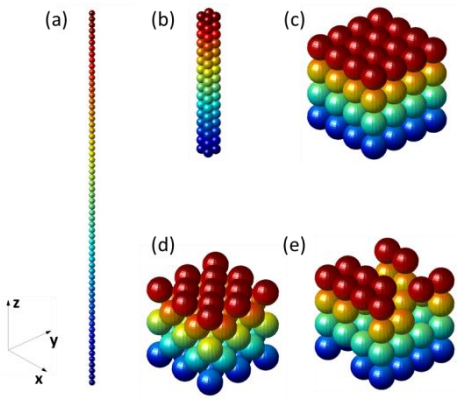

Figure 1. Stereographic view of sample of chain cluster (a), cylinder cluster (b), and cube culsters with simple cubic (c), FCC (d) and defected lattice (e). The lattice vectors keep parallel to the X, Y and Z axis. The positive directin of Z axis is aligned with the direction of [001].

The process of simulation starts with a thermalization at zero field from high temperature and to 300 K. And then, the magnetic field is applied and increased in small intervals until the field amplitude H_0; then it is decreased down to $-H_0$, and increased again up to H_0 so that the cycle is complete. The time-depend magnetization was proceed through Monte Carlo method and the well-known Metropolis algorithm[32]. In the first place, one particle is picked randomly within the cluster. Next, the particle moment is directly agitated to a new orientation chosen inside of a spherical segment around the present orientation with an aperture angle $\delta\theta$. According to the reported work[16], the temperature dependence of $\delta\theta$ is given by $\delta\theta = a(0.05 \times k_B T / 2K_{eff} V) \wedge 0.5$ in the usual reduced unit, where a is used to alter the value of $\delta\theta$ for accuracy adjustment of simulation, and k_B is the Boltzmann constant. This agitation is accepted with probability min $[1, \exp(-\Delta E / k_B T)]$, where ΔE is the change in the total energy of cluster system caused by the agitation, and T is the temperature kept at 310 K (body temperature). The above procedure is repeated until all particles are agitated, and this is defined as one Monte Carlo (MC) step. The magnetization of the system is recorded by collecting projections of the particle moments along the field direction at each time when the phase of the magnetic field varied by 0.9 degree (the interval of field variance). During the simulation, the particles only relax through Nèel mechanism. To reproduce the M-H curve of cluster, the cycle is repeated for at least 200 times, and the final curve is gained by averaging over the result of each cycle.

We adjust simulation accuracy by equating the loss per cycle of 64 non-interacting SPMNs obtained from simulation with the result of calculation by classic theory of Rosensweig describing the magnetic hystereisis of non-interacting SPMNs under an oscillating field[5]. When the particles don't magnetically interact with each other, the loss per cycle per unit volume of magnetic material

has nothing to do with the manner of the spacial arrangement of particles. So the accuracy of simulation maintains regardless of the morphology or structure of particle assembly. The field frequency f and amplitude H_0 used in the calculation are set to be 300 kHz and 200 kA/m respectively, and both in range practically used [33]. The loss per cycle gained from simulation is adjusted by changing the value of $\delta\theta$ and the amount of MC step per field variance interval. Here, the relative deviation is used to determine the degree of accuracy, which is defined as $\frac{|A_{simu}-A_{theo}|}{A_{theo}}\times 100\%$, where A_{simu} and A_{theo} is the loss per cycle per unit volume of magnetic material gained from simulation and calculation by Rosensweig's theory respectively. Figure 2 shows the plot of $\delta\theta$ -dependent relative deviation as function of the amount of MC step per interval. A maximum similarity between simulation and calculation exists, which shifts to the low number of MC step per interval during increasing $\delta\theta$. Considering saving simulation time, 50 MC steps per interval and $a = 2$ are selected for all of simulations.

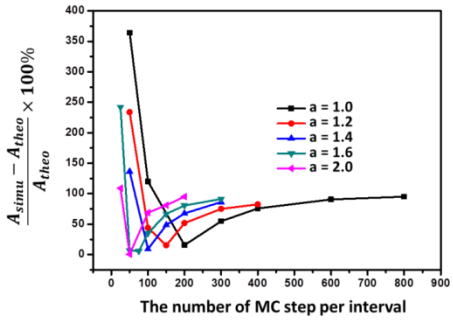

Figure 2. The plot of the relative deviation of loop per cycle of non-interacting SMNPs obtained from between simulation and Rosensweig's calculation as a function of the number of Monte Carlo step per interval at a =1.0, 1.2, 1.4, 1.6, and 2.0.

The accuracy of simulation running on cubic cluster with FCC lattice is not re-adjusted because of the similar number of particle in the cluster. In order to maintain the accuracy of simulation cubic clusters with defected lattice, the agitations of their magnetic moments are still involved in every MC step, but their contributions to the inter-particle dipole interactions and the magnetization of the cluster system are both omitted.

3. Definition of tendency of cluster to remain magnetically aligned with a field

When the particles' moments get aligned with a magnetic field, the dipole energy equation (3) can be simplified to,

$$E_D^{(i,j)} = \frac{\mu_0 M_d^2 V^2}{4\pi}\left[\frac{1-3\left(\cos\theta_{ij}\right)^2}{r_{ij}^3}\right] \qquad (5)$$

where θ_{ij} is the angle between the direction of the magnetic field and the line joining the centres of the particle i and j . All of parameters outside of the bracket are constants. By summing up $\frac{1-3\left(\cos\theta_{ij}\right)^2}{r_{ij}^3}$ over all of pairs of particles of cluster, $\sum_{i<j}\frac{1-3\left(\cos\theta_{ij}\right)^2}{r_{ij}^3}$ determines the total energy of dipole interactions when the cluster is magnetically aligned with the field. The lower $\sum_{i<j}\frac{1-3\left(\cos\theta_{ij}\right)^2}{r_{ij}^3}$, the more table dipole interactions will be gained when particles aligned with the field, and the larger tendency of particles to remain aligned with the field orientation. A positive $\sum_{i<j}\frac{1-3\left(\cos\theta_{ij}\right)^2}{r_{ij}^3}$ indicates that the cluster is less inclined to remain magnetically aligned with the field orientation. Therefore, we use $\sum_{i<j}\frac{1-3\left(\cos\theta_{ij}\right)^2}{r_{ij}^3}$ to evaluate the tendency of cluster to remain magnetically aligned with a field.

2. Results and discussion

To increase the stability of modelling, the cluster systems investigated in this study undergo a long-term of thermalization from high temperature to 300 K. After the

thermalization all the cluster systems achieve completely relaxed. The coercivity is zero, in other words, the moments are orientated randomly in space.

Clusters characteristics and simulation results are summarized in Table 1. The morphology anisotropy of cluster along the field axis is evaluated by the aspect ratio of length of cluster in the field orientation to the width perpendicular to the field orientation. If this parameter is close to 1, the cluster exhibits less anisotropy in shape along the field orientation. The positive direction of field axis is used to define the orientation of field axis. N_{omit} shows the number of particle missed in cluster lattice. The loop area A_{loop} of M-H curve represents the loss per cycle per unit volume of magnetic material gained from the calculation of absolute value of integration of magnetization against field intensity. The slope peak of M-H curve, $Peak_{slope}$, is obtained by averaging the maximums of dual peaks of the gauss fitting curve of the slope at each interval of field variance. Given by a fixed saturation magnetization, $Peak_{slope}$ can be used to assess the difficulty of cluster been magnetised. Coercivity is the field intensity at which the magnetization of cluster decreases to 0, indicating the hardness of cluster being demagnetised.

Figure 3 shows the results of simulations running on chain, cylinder and cube cluster with simple cubic lattice. In the cases that the aspect ratio of length of cluster in the field orientation to the width perpendicular to the field orientation is equal to 64, 8 and 1, the magnetic field varies along the axis with positive direction of [001]. To reduce this aspect ratio to 0.125 and 0.016, the field axis applied in the simulations of cylinder and chain changes to the one with positive direction of [100]. It can be seen that all of M-H curves possess clear hysteresis loop (Figure 3a). As shown in figure 3b, A_{loop} increases sharply from 2.11 to 20.13 kJ/m^3 when the aspect ratio of length of cluster in the field orientation to the width perpendicular to the field orientation increases from 0.016 to 64. At the same time the coercivity increases from 2.81 to 13.27 kA/m, indicating that the demagnetisation is becoming harder. The increased $Peak_{slope}$ with the aspect ratio (Figure 3c) tells that an easier magnetization occurs. The decrease of $\sum_{i<j}\frac{1-3\left(\cos\theta_{ij}\right)^2}{r_{ij}^3}$ from 75 to -150 (Figure 3d) suggests that the cluster is more likely to remain magnetically aligned with the field orientation. Therefore, the magnetic hysteresis of cluster is enlarged, as well as the loss per cycle. Otherwise, it seems that the heating ability of cluster can exceeds non-interacting SMNPs as long as the aspect ratio of length in the field orientation to the width perpendicular to the field orientation is below 3 (Figure 3b). So, the advantage of assembling the particles into cluster may be damaged when the particles form a cluster with less anisotropy in shape, which is in agreement with the experimental results reported by Liu *et al*., who found a reduction in heating ability when SMNPs were high-contently loaded into a sphere-like polymer latex[22].

To further confirm the impact of morphology anisotropy on heating efficiency of SMNP clusters, the simulations running on cube clusters with simple cubic and FCC lattice along other field axes are performed, including ones with positive directions of [110],[111],[111] and [112] (illustrated in Figure 4a). Table 1 shows that the $\sum_{i<j}\frac{1-3\left(\cos\theta_{ij}\right)^2}{r_{ij}^3}$ when the clusters are magnetically aligned along these orientation are found to be nearly zero regardless of the type of lattice. The zoom-in M-H curves of cube cluster with simple cubic driven by the fields varying in these orientations and the corresponding gauss fitting curves of slope against field intensity are given in Figure 4a and b. As a benchmark, the M-H curve of cube cluster driven by the magnetic field varying in the axis with positive direction of [001] is also included. It can be seen that these four M-H curves are almost the same and possess similar coercivity with an average value and a relative standard deviation of 2.89 kA/m (± 2.98%), loop area of 4.01 J/m^3 (± 0.35%) and $Peak_{slope}$ of 7.33 (±

1.27%). And the change of simple cubic to FCC lattice even does not alter the magnetic hysteresis much. The coercivity varies to 2.97 kA/m (± 3.91%), loop area to 3.91 J/m^3 (± 2.79%) and $Peak_{slope}$ to 7.30 (± 1.59%).

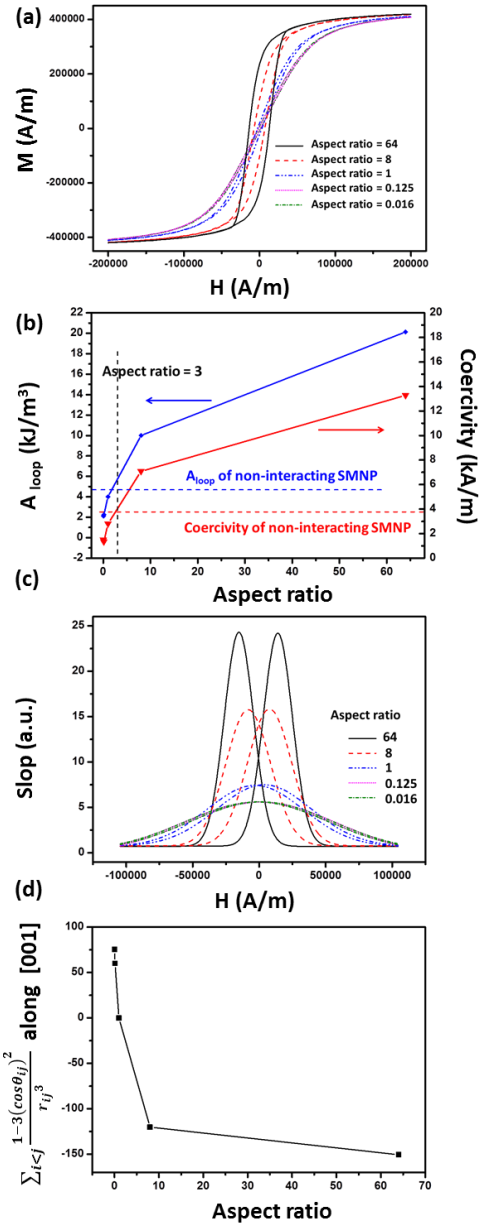

Figure 3. (a) The simulation M-H curves under AC magnetic field varying along the axis with positive direction of [001] when aspect ratio =0.016, 0.125, 1, 8 and 64. (b) The plots of loop area A_{loop} and coercivity as a function of aspect ratio. (c) Gauss fitting curve of the slope-H of M-H curve. (d) The plot of $\sum_{i<j}\frac{1-3(\cos\theta_{ij})^2}{r_{ij}^3}$ as a function of aspect ratio.

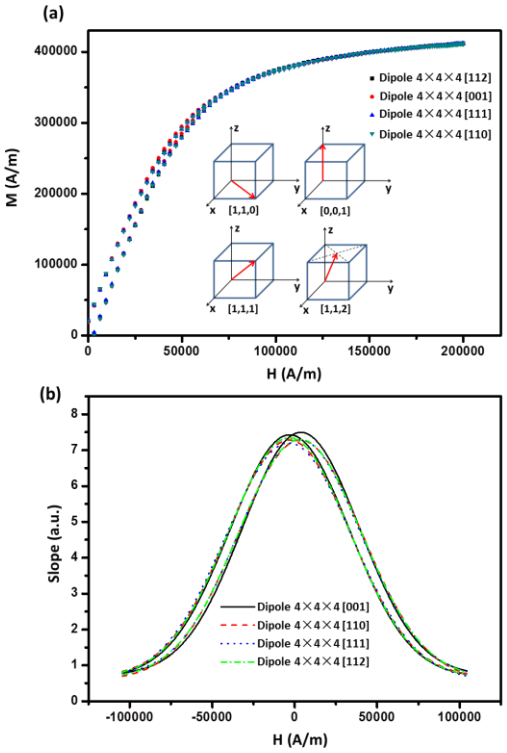

Figure 4. (a) Zoom-in simulation M-H curves of cube cluster with simple cubic lattice driven by magnetic fields varying along axes with positive directions of [110], [001], [111] and [112] and (b) their slope-H gauss fitting curves. Insert: Illustrations of directions of [110], [001], [111] and [112], which are represented by red arrows.

While the clusters with high morphology anisotropy seem to be with great potential for hyperthermia, at present the synthesis of shape-anisotropic-less SMNP clusters have been studied widely, and many facile methods have been developed to controllably and massively prepare SMNP clusters sphere-like in shape with ordered and disordered structure[34-36]. Now that the cube clusters with ordered structure show little advantage in hyperthermia heating as discussed before, here we intend to study whether introducing defects to the lattice will favor the heating efficiency. 50000 clusters with defected lattice are

fabricated by omitting 16 randomly-picked particles from the lattice of cube cluster with simple cubic. As a results, the $\sum_{i<j}\frac{1-3\left(\cos\theta_{ij}\right)^2}{r_{ij}^3}$ flocculates within the range from -20 to 25 when these clusters are magnetically aligned along [001] direction. Figure 5 gives the probability distribution for a certain $\sum_{i<j}\frac{1-3\left(\cos\theta_{ij}\right)^2}{r_{ij}^3}$ to appear. It can be seen that probabilities to reduce and increase the tendency of cluster to remain aligned with [001] direction are almost the same. 10 clusters with defected lattice are picked out for simulation driven by the field varying in the axis with positive direction of [001]. We find that both $Peak_{slope}$ and A_{loop} decrease with the $\sum_{i<j}\frac{1-3\left(\cos\theta_{ij}\right)^2}{r_{ij}^3}$ when the clusters are magnetically aligned along [001] direction. However, the coercivity flocculates within the range from 2.7 to 3.3 kA/m (see Table 1). Therefore, without strong morphology anisotropy along the filed axis, the magnetic hysteresis of cluster is controlled by the difficulty to be magnetised.

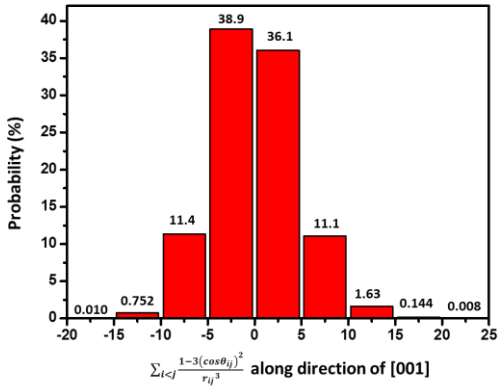

Figure 5. Histogram of the probability distribution for $\sum_{i<j}\frac{1-3\left(\cos\theta_{ij}\right)^2}{r_{ij}^3}$ when the cube clusters with defected lattice are aligned with direction of [001].

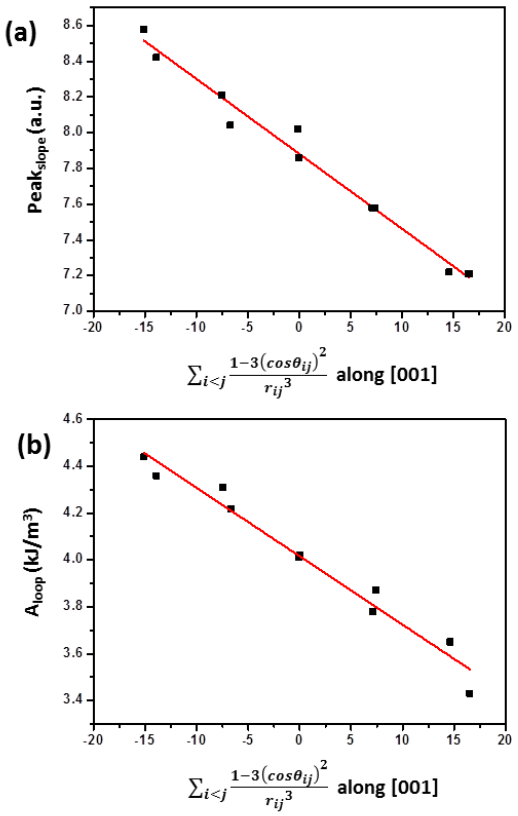

Figure 6. The plots of the $Peak_{slope}$ (a) and A_{loop} (b) of 10 cube clusters with defected lattice as a function of $\sum_{i<j}\frac{1-3\left(\cos\theta_{ij}\right)^2}{r_{ij}^3}$ obtained when cluster is magnetically aligned with [001] direction.

To offer a full-scope conclusion about the heating ability of cube cluster with defected lattice, we average the probability of appearance of $\sum_{i<j}\frac{1-3\left(\cos\theta_{ij}\right)^2}{r_{ij}^3}$ over 1000 field orientations (illustrated in Figure 7a) base on these 50000 clusters with defected lattice. As shown in Figure 7b, while the range of distribution is enlarged, the profile of distribution shows little different from the case that the clusters are aligned with [001] direction. Based on the simulation results gained by now, assembling SMNP into cluster with less anisotropy in shape may make the heating efficiency numb to the manipulation of the cluster properties.

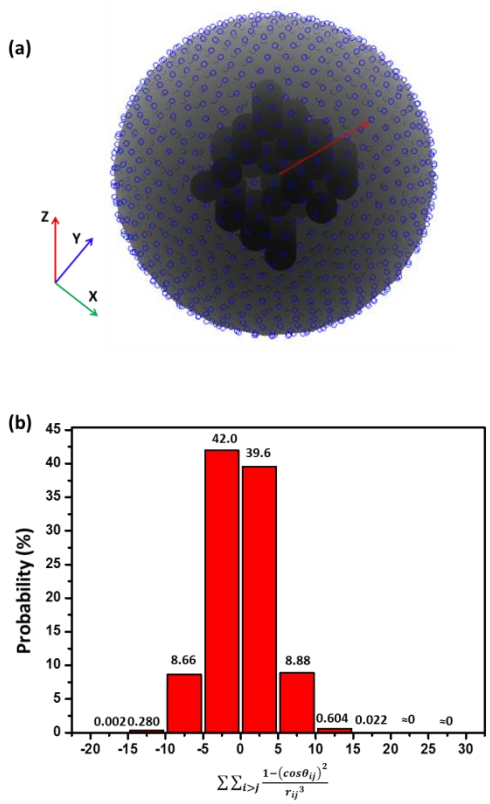

Figure 7. (a) Illustraion of the distribution of 1000 field orientaions. Each line connecting the centre and point on the surface of the sphere represents a field orientation. (b) Histogram of the average probability distribution over 1000 field orientations for $\sum_{i<j}\frac{1-3(\cos\theta_{ij})^2}{r_{ij}^3}$ of cube cluster with defected lattice.

2. Conclusion

In this work, we study, by Monte Carlo simulations, the influence of morphology anisotropy of SMNP clusters on the magnetic hysteresis in the way changing the tendency of cluster to remain magnetically aligned with a certain field orientation. A specific way is applied to evaluate this tendency of cluster via discussing the energy of inter-particle dipole interactions when the particles are aligned with a field. Clusters with three types of shape are investigated, including chain, cylinder and cube. When the aspect ratio of the length of cluster in the field orientation to the width perpendicular to the field orientation is enlarged, clusters are more likely to remain aligned with the field orientation because of the lowered energy of dipole interactions. Thus, the magnetic hysteresis of cluster is enhanced, so does the heating efficiency. Without strong morphology anisotropy like cube cluster, changes in lattice type alter the magnetic hysteresis little because the tendency of cluster to remain magnetically aligned with the field orientation remains the same. Introduction of defect to the lattice can make the loss per cycle flocculated within a range, but the probability to increase or decrease the magnetic hysteresis is roughly the same regardless of the selection of field orientation. Actually, in a liquid suspension, particles undergo aggregations more or less[37, 38], and after being injected to the tumor, the conglomeration of particle is always unavoidable[25]. So the study of the relationship between the properties of cluster and heating efficiency is urgent. To explain the results published on the induction heating of MNP clusters, we still have a long way to go.

ACKNOWLEDGEMENTS

REFERENCES

[1] R. Hergt and S. Dutz, J. Magn. Magn. Mater. **311**, 187 (2007).
[2] Q. A. Pankhurst, N. T. K. Thanh, S. K. Jones, and J. Dobson, J. Phys. D: Appl. Phys. **42**, 224001 (2009).
[3] J. P. Reilly, *Applied Bioelectricity: from Electrical Stimulation to Electropathology* (Springer New York, 1998).
[4] J.-P. Fortin, C. Wilhelm, J. Servais, C. Ménager, J.-C. Bacri, and F. Gazeau, J. Am. Chem. Soc. **129**, 2628 (2007).
[5] R. E. Rosensweig, J. Magn. Magn. Mater. **252**, 370 (2002).
[6] H. Rudolf, D. Silvio, M. Robert, and Z. Matthias, J. Phys.: Condens. Matter **18**, S2919 (2006).
[7] G. Vallejo-Fernandez, O. Whear, A. G. Roca, S. Hussain, J. Timmis, V. Patel, and K. O. Grady, J. Phys. D: Appl. Phys. **46**, 312001 (2013).

[8] M. Kallumadil, M. Tada, T. Nakagawa, M. Abe, P. Southern, and Q. A. Pankhurst, J. Magn. Magn. Mater. **321**, 1509 (2009).
[9] M. Ma, Y. Wu, J. Zhou, Y. Sun, Y. Zhang, and N. Gu, J. Magn. Magn. Mater. **268**, 33 (2004).
[10] A. H. Habib, C. L. Ondeck, P. Chaudhary, M. R. Bockstaller, and M. E. McHenry, J. Appl. Phys. **103**, 07A307 (2008).
[11] J.-H. Lee, et al., Nature Nanotech. **6**, 418 (2011).
[12] J.-t. Jang, H. Nah, J.-H. Lee, S. H. Moon, M. G. Kim, and J. Cheon, Angew. Chem. Int. Ed. **48**, 1234 (2009).
[13] P. Guardia, R. Di Corato, L. Lartigue, C. Wilhelm, A. Espinosa, M. Garcia-Hernandez, F. Gazeau, L. Manna, and T. Pellegrino, ACS Nano **6**, 3080 (2012).
[14] C. Martinez-Boubeta, et al., Sci. Rep. **3** (2013).
[15] H. Mamiya and B. Jeyadevan, Sci. Rep. **1** (2011).
[16] D. Serantes, et al., J. Appl. Phys. **108**, 073918 (2010).
[17] K. Eiji, et al., J. Phys. D: Appl. Phys. **43**, 474011 (2010).
[18] E. Kita, et al., J. Appl. Phys. **107** (2010).
[19] H. Rudolf, D. Silvio, and R. Michael, J. Phys.: Condens. Matter **20**, 385214 (2008).
[20] H. Rudolf, D. Silvio, and Z. Matthias, Nanotechnology **21**, 015706 (2010).
[21] N. M. Hayashi K, Sakamoto W, Yogo T, Miki H, Ozaki S, Abe M, Matsumoto T, Ishimura K, Theranostics **3**, 366 (2013).
[22] X. L. Liu, et al., J. Mater. Chem. B **2**, 120 (2014).
[23] S. Dutz, J. H. Clement, D. Eberbeck, T. Gelbrich, R. Hergt, R. Müller, J. Wotschadlo, and M. Zeisberger, J. Magn. Magn. Mater. **321**, 1501 (2009).
[24] S. A. Gudoshnikov, B. Y. Liubimov, and N. A. Usov, AIP Advances **2** (2012).
[25] C. L. Dennis, A. J. Jackson, J. A. Borchers, P. J. Hoopes, R. Strawbridge, A. R. Foreman, J. v. Lierop, C. Grüttner, and R. Ivkov, Nanotechnology **20**, 395103 (2009).
[26] F. Burrows, C. Parker, R. F. L. Evans, Y. Hancock, O. Hovorka, and R. W. Chantrell, Journal of Physics D: Applied Physics **43**, 474010 (2010).
[27] J. Faraudo, J. S. Andreu, and J. Camacho, Soft Matter **9**, 6654 (2013).
[28] B. Mehdaoui, R. P. Tan, A. Meffre, J. Carrey, S. Lachaize, B. Chaudret, and M. Respaud, Phys. Rev. B **87**, 174419 (2013).
[29] T. Wang, D. LaMontagne, J. Lynch, J. Zhuang, and Y. C. Cao, Chemical Society Reviews **42**, 2804 (2013).
[30] Y. Lu, L. Dong, L.-C. Zhang, Y.-D. Su, and S.-H. Yu, Nano Today **7**, 297 (2012).
[31] J. García-Otero, M. Porto, J. Rivas, and A. Bunde, Phys. Rev. Lett. **84**, 167 (2000).
[32] W. Figueiredo and W. Schwarzacher, Phys. Rev. B **77**, 104419 (2008).
[33] A. Jordan, et al., J. Magn. Magn. Mater. **225**, 118 (2001).
[34] Z. Lu and Y. Yin, Chem. Soc. Rev. **41**, 6874 (2012).
[35] R. Fu, X. Jin, J. Liang, W. Zheng, J. Zhuang, and W. Yang, J. Mater. Chem. **21**, 15352 (2011).
[36] T. Wang, D. LaMontagne, J. Lynch, J. Zhuang, and Y. C. Cao, Chem. Soc. Rev. **42**, 2804 (2013).
[37] M. Klokkenburg, C. Vonk, E. M. Claesson, J. D. Meeldijk, B. H. Erné, and A. P. Philipse, J. Am. Chem. Soc. **126**, 16706 (2004).
[38] K. Butter, P. H. H. Bomans, P. M. Frederik, G. J. Vroege, and A. P. Philipse, Nature Mater. **2**, 88 (2003).

Table 1. Summary of SMNP clusters characteristics and simulation results.

sample	Positive direction of field axis	N_{omit}	$\sum_{i<j}\frac{1-3(\cos\theta_{ij})^2}{r_{ij}^3}$	Aspect ratio	Coercivity (kA/m)	$Peak_{slope}$ (a.u.)	A_{loop} (kJ/m^3)
Non interaction	[001]	0	-	-	3.77	9.70	4.69
1×1×64	[001]	0	-150.6	64	13.27	24.24	20.13
1×1×64	[100]	0	75.3	0.016	1.50	5.61	2.11
2×2×16	[001]	0	-120.2	8	7.08	15.79	10.01
2×2×16	[100]	0	60.0	0.125	1.33	5.60	2.25
FCC 63	[001]	0	≈0	1	2.91	7.44	3.95
FCC 63	[111]	0	≈0	1	3.08	7.21	3.82
FCC 63	[110]	0	≈0	1	2.84	7.20	3.83
FCC 63	[112]	0	≈0	1	3.06	7.35	4.05
4×4×4	[001]	0	≈0	1	2.81	7.46	4.00
4×4×4	[111]	0	≈0	1	2.82	7.25	4.03
4×4×4	[110]	0	≈0	1	2.99	7.28	4.01
4×4×4	[112]	0	≈0	1	2.92	7.32	4.00
4×4×4	[001]	16	-15.1	≈1	3.18	8.58	4.44
4×4×4	[001]	16	-7.5	≈1	3.28	8.21	4.31
4×4×4	[001]	16	-0.1	≈1	3.15	8.02	4.01
4×4×4	[001]	16	7.4	≈1	3.05	7.58	3.87
4×4×4	[001]	16	16.5	≈1	2.89	7.21	3.43
4×4×4	[001]	16	-13.9	≈1	2.97	8.42	4.36
4×4×4	[001]	16	-6.7	≈1	3.08	8.04	4.22
4×4×4	[001]	16	≈0	≈1	3.18	7.86	4.02
4×4×4	[001]	16	7.1	≈1	2.72	7.58	3.78
4×4×4	[001]	16	14.6	≈1	3.05	7.22	3.65